Dating of a ring on one of the largest known Roman iron anchors (La Grande-Motte, France): Combined metal and organic material radiocarbon analysis

Sébastien Berthaut-Clarac, Emmanuel Nantet, Stéphanie Leroy, Emmanuelle Delque-Količ, Marion Perron, Pierre Adam, Philippe Schaeffer, Céline Kerfant

Dating of a ring on one of the largest known Roman iron anchors (La Grande-Motte, France): combined metal and organic material radiocarbon analysis

Authors and affiliations: Sébastien Berthaut-Clarac[a], Emmanuel Nantet[b], Stephanie Leroy[c], Emmanuelle Delqué-Količ[d], Marion Perron[d], Pierre Adam[e], Philippe Schaeffer[e], Céline Kerfant[f]

[a] Centre de Recherche sur les Sociétés et Environnements en Méditerranée (CRESEM) UR7397, University of Perpignan *Via Domitia* (UPVD), 52 avenue Paul Alduy, 66860 Perpignan Cedex 9, France bc.sebastien@gmail.com https://orcid.org/0000-0002-8304-5903

[b] University of Haifa, Department of Maritime Civilizations, The Leon Recanati Institute for Maritime Studies, Laboratory for Nautical Archaeology and History, Israel. Abba Khoushy Ave 199, 3498838 Haifa, Israel. enantet@univ.haifa.ac.il https://orcid.org/0000-0002-0003-6615

[c] LAPA-IRAMAT, NIMBE, CEA, CNRS, Université Paris-Saclay, CEA Saclay, 91191 Gif-sur-Yvette France. stephanie.leroy@cea.fr ,

[d] Laboratoire de Mesure du Carbone 14 (LMC14), LSCE/IPSL, CEA-CNRS-UVSQ, Université Paris-Saclay, 91191 Gif-sur-Yvette, France. emmanuelle.delque-kolic@cea.fr, marion.perron@cea.fr

[e] Université de Strasbourg, CNRS, Institut de Chimie de Strasbourg UMR7177, 4 rue Blaise Pascal, 67000 Strasbourg, France. padam@unistra.fr, p.schaef@unistra.fr

[f] Researcher associate, Institut Català de Paleoecologia Humana i Evolució Social (IPHES-CERCA), Zona Educacional 4, Campus Sescelades URV (Edifici W3), 43007 Tarragona, Spain, and Universitat Rovira i Virgili, Departament d'Història i Història de l'Art, Avinguda de Catalunya 35, 43002 Tarragona, Spain ckerfant@iphes.cat

Abstract

Underwater operations conducted along the southern French coast have unveiled two large, isolated anchors of iron. The largest ever found in the ancient Mediterranean, they reveal that Roman merchantmen moored in Aigues-Mortes Bay. A combination of analyses focusing on the ring, which belonged to one of the two anchors, offered the opportunity to collect data from isolated anchors and to document their production. Radiocarbon analysis, conducted for the first time on this type of object, determined that they were manufactured in the early imperial period. Another key discovery was a layer of fibers found in a concretion from the ring, which revealed rare remnants of ropes impregnated with pitch that could correspond to puddening. The replication of similar analyses on rings belonging to other anchors would provide a better understanding of this crucial component for ancient mooring.

keywords: large iron anchors; ring; puddening; radiocarbon analysis; fibers; pitch

1 Introduction

Two iron anchors found in La Grande-Motte (Hérault) reveal significant dimensions. Their discovery and subsequent examination are not supported by additional archaeological contexts that could assist in dating. Anchoring is an important topic for historical examination as the manufacturing of these devices involves advanced skills and many resources, which had significant economic consequences as a result. So far, earlier studies dedicated to anchors have mostly focused on their material and shape especially their arms and stock that could produce a chrono-typology (Moll, 1927; Frost, 1970 for the stone-anchors; Kapitän, 1984; Haldane, 1986a, 1986b; Frost, 1997; Votruba, 2019). More recently, research has focused on assessing the provenance of ancient anchors, notably through isotopic studies of lead stock (Kuleff, 1995), and the radiocarbon dating of preserved wood from the same typology of anchors (Hadas, 2005). Archaeometric studies have been carried out on iron anchors to uncover the manufacturing methods (among others, Samuels, 1980; Light, 1992; Eliyahu, 2011; Ciarlo, 2011).

However, none of these analyses established the dating of the iron anchors by any other parameter aside from typology. Our paper presents a new methodology to establish dating in order to confirm that the iron anchors from La Grande Motte are the largest ancient iron anchors to have ever been found. In addition, the analyses carried out on the ring and its concretion have brought to light probable remains of fibers, which can be dated to the same period as the manufacturing of the iron anchor.

2 The anchors: location, finds, context, and characteristics

2.1 Location of the anchors

The anchors were found in 2016 at La Grande-Motte, a port built in 1965 in an uninhabited place in the Aigues-Mortes Bay, the easternmost part of the coast before the Rhône delta (Figure 1). The shore is made up of wetlands and includes numerous lagoons that once connected the ancient settlements flourishing in the hinterland to the sea with short natural channels called "*grau*." So far, no evidence of ancient occupation has been found within the town, unlike the territory bordering the marshes to the north of the port. The bay located along the coast of Gallia Narbonensis probably belonged to a segment of an important maritime route. In a favorable location, it was situated between the Roman settlements of Agatha (Agde), Nemausus (Nîmes), and Arleat (Arles), which constituted significant economic poles. Even closer to the bay is the ancient harbor of Lattara (Lattes) that reached its peak of occupation in the 1st cent. CE (Jorda et al., 2008; Bagan et al., 2010; Steiner et al., 2020). Despite this strategic position, the bay has not revealed many underwater finds. The most significant ancient underwater remains discovered in this area were located 5 km away and consisted of drums and lithic building materials (Jézégou, forthcoming). The stone cargo largely came from a quarry located to the north, in Bois de Lens (Gard). Actively exploited in the early imperial period (Bessac, 2002), these finds demonstrate that vessels most likely sailed into this bay from the area north of the marshes.

2.2 Isolated anchors

The magnetometric surveys supervised by M. Guérout (Guérout 2018) that led to the discovery of the anchors were aimed initially at searching for the wrecks of five Genoese merchantmen that sank in 1165 near the grau de Melgueil. Instead, it resulted in the detection of five iron anchors, including the two large examples that are the focus of our investigation. They were found isolated and devoid of additional archaeological contexts such as remains of the hull of a ship or cargo. The three probes (C1, C2 and C3 in Figure 2) uncovered two anchors broken into five fragments lying on the rock seafloor under 0.7 m of sediment, mainly consisting of sand and silt. Further operations conducted in the bay of Aigues-Mortes evidenced three more iron anchors to the south deprived of any stock, in addition to a lead stock

1.88 m long, belonging to the 3b type as defined by Kapitän (1984) and habitually in use from the 3rd cent. BCE to the 1st cent. CE.

2.3 Characteristics of the anchors

The two large iron anchors are remarkable for their very large size (Table 1). They had been broken down into five pieces (Figure 3). Pieces C1/1 and C3/1 correspond to the upper part of a shank with their stocks, also of iron, still set into the latter. We have identified fragments C2 and C3/2 respectively to be the lower part of the anchors, which included the arms. It is worth noting that the shanks of both anchors have been fractured at the very same place, 117 and 116 cm from their crowns (all measurements were taken at the lowest point of the concretions). The fifth piece, which is straight in its general form, is probably the remnant of a stock (C1/2). Fragments C1/1, C1/2, and C2 came most likely from the same anchor, whereas C3/1 and C3/2 belong to another example.

The remnants of the shanks are 375 and 370 cm long (given both shanks are broken). Beyond their very large size, the two shanks reveal strong resemblances: their rectangular sections are almost square and of equal dimensions (19 x 17 cm). Their arm-beams are 185 cm in length for the first and 180 cm for the second. The rings demonstrate corresponding measurements: 32 and 35 cm respectively for the outer diameter and 24 and 23 cm for the inner diameter. These similarities indicate that the upper and lower parts of the shank, including its arms, were likely produced using the same technique and could belong to one or two separate vessels of similar size. Even so, their stocks are quite different: that of the first anchor is longer than 293 cm with a 11 x 6 cm rectangular section. The length of the second is 228 cm, and it has a 13 x 12 cm rectangular section. The stocks of both anchors probably slipped inside the shank, which might explain why they are longer on one side than on the other but a break is not to be excluded. The lower extremities of the two mooring devices had a crown that does not seem to have been provided with a second ring (the first and principal was that at the top of the shank). Both anchors belong to the type B as defined by Kapitän (1984) and were provided with round-shaped arms, which was a very common typology in the early imperial period.

3 Materials and methods

The ring was the key component of the anchor, and thus our present investigation analyzes it carefully. The C3/1 assembly was pieced together on a barge, and we cut the ring with a circular saw on either side of the shank (Figure 4). The C3/1 assembly was then re-immersed exactly in its position and re-sanded according to the DRASSM (Département des Recherches Subaquatiques et Sous-Marines) instructions. Surprisingly, both cut ends revealed bright surfaces of metal, when the metal within a concretion is usually found to be far more degraded. After cleaning part of the concretions, a thin black

120 layer mixed with fibers could be observed adhering to the metallic surface. We postulate that this deposit
121 could correspond to the remains of a rope coated with pitch that was wrapped around the ring, the so-
122 called puddening, since this is what the shape of the concretion would suggest. Our analysis relied on a
123 set of techniques conducted on the metal structure of the ring as well as on the black layer and the fibers
124 that are described below in further detail. The aim was to identify the materials employed and to obtain
125 the date range using ^{14}C on the fibers and on the metal by means of an innovative combination of
126 methods of analysis.
127

128 ### 3.1 **Radiocarbon dating of the iron from the ring**

129

130 Radiocarbon dating of iron produced by the bloomery process is viable since the carbon contained in
131 the steely zones of the metal came from charcoal used as a fuel during the smelting process (Van der
132 Merwe and Stuiver, 1968). Within the furnace, the carbon from charcoal and from the CO resulting from
133 its combustion is incorporated into the metal by means of diffusion. Carbon is hence heterogeneously
134 distributed within the metallic matrix, ranging from very low contents (< 0.02 wt % C) to higher values
135 of 0.8 wt % C.
136

137 Several authors have demonstrated that sources of carbon of different origins can contribute to the
138 misdating of iron (for example, see Craddock et al., 2002, Hüls et al., 2011). By applying an approach
139 based on accelerator mass spectrometry (AMS), coupled with a metallographic study and an adequate
140 sampling process, it was recently shown that a reliable radiocarbon dating of the iron can be determined
141 (Delqué-Količ et al., 2016; Leroy et al., 2015a, 2015b). This study consists of two decisive stages of
142 investigation in order to document the nature of the metal and to avoid any risks of misdating (recycling
143 process, presence of exogenous carbon, measurement of a quantity of carbon below the detection limit).
144 This method aims at determining the nature of the smelting process, identifying the manufacturing
145 process used by the blacksmith to forge the object (assembly or not of different metal pieces), and
146 detecting the most carburized areas in the metal to extract enough carbon for the ^{14}C measurement. Thus,
147 if this study makes it possible to obtain crucial data on the manufacturing process of the object, a
148 prerequisite for reliable ^{14}C dating, it does not seek to characterize the choices and technical gestures
149 made by the blacksmith or the origin of the metal in detail.
150

151 Full details of the approach in Leroy et al. (2015b), only the most important steps are reported here. A
152 large specimen was sampled at the less corroded cut end of the ring before being cross-sectioned and
153 polished with abrasive paper and diamond paste (3 to 1 µm grain size), which are the usual techniques
154 for the preparation of iron for the exposition of the metallic matrix of the samples. Then, a
155 metallographic exam of the metal (3% Nital etching, Oberhoffer's reagent) was conducted to reveal the

carbon content within the metal, and to visualize the possible welding lines, possibly pointing to the assembly of different metal pieces and to the possible recycling of old iron.

The elemental analysis of the Slag Inclusion (SI) entrapped in the metal also assists in providing pertinent information about the manufacturing of the object, such as the detection of any potential recycling after the initial smelting process (Leroy et al., 2015b). Indeed, a set of major elemental compounds of the ore that are not reduced during smelting (mainly Al_2O_3, SiO_2, K_2O, CaO and MgO) have in most cases a constant elemental ratio in the SI of each iron artifact (Dillmann and L'Héritier, 2007; Buchwald and Wivel, 1998). The signature of a smelting operation with the same ore, charcoal, fluxes, and furnace lining can thus be identified through the comparison of the ratios of elements contained in the SI. When recycled, old iron can be used and welded with other pieces to produce the final object. The iron artifacts containing separate pieces of different constant ratios can be detected in their SI and, therefore, various signatures can be identified within a sample. To compare the ratios values and identify the chemical signature(s) within the sample, we used multivariate analyses (Principal Component Analysis (PCA) and cluster analysis) following the approach detailed in Disser et al. (2014). The statistical analysis is based on a scale invariant representation of the element's concentration, which is obtained by dividing the concentration of all elements by the geometrical mean of the set of measured elements as the internal standard (Leroy et al., 2012, Disser et al., 2014). The use of multivariate analysis, such as PCA, is a way to consider simultaneously all the ratios values to detect variabilities and differences. Prior to sampling for radiocarbon measurements, the compositional investigation of the SI was thus carried out.

Following our observations, samples for AMS were collected within the expected highest carburized zones of the metal with a 3 mm-diameter metallic drill coated with cobalt boron (CoB) to obtain approximately 1 mg of carbon for ^{14}C dating. The resulting samples were combusted to CO_2 according to the conditions detailed in Leroy et al. (2015b), and the CO_2 samples were graphitized at the LMC14 laboratory as described in Delqué-Količ et al. (2016). The ^{14}C measurements were carried out by "ARTEMIS," an AMS facility located in Saclay (France) (Moreau et al., 2013).

3.2 Analyses and radiocarbon dating of the black layer and fibers

Very small fibers were visible within the black layer, and examination under a digital microscope (Dino-Lite AM7915MZTL) confirmed the presence of submillimetric fibers impregnated with a brown to dark matter (Figure 5).

3.2.1 Fiber preparation for SEM analysis

The microbotanical remains were investigated with the scanning electron microscope (SEM) Neoscope Philips XL 30 CP. As the remains suffered a mineralization process, the samples were placed on an adhesive carbon disc without any further action. The SEM provides high resolution pictures of up to a nanometer of the surface of the sample surface and is therefore an effective tool to obtain the basic data for establishing a taxonomic identification.

3.2.2 Analytical procedure for the organic molecular investigation of pitch and fibers

3.2.2.1 Extraction with organic solvents

A small quantity of the black layer (984 mg) visible within the concretion was collected by scraping with a metal spatula. The sample was extracted by sonication (20 min) with a mixture of dichloromethane (DCM) and methanol (MeOH) (1:1 v/v; 30 ml). The solvent extract (22.5 mg) was recovered after centrifugation and removal of the solvents under reduced pressure.

3.2.2.2 Derivatization and fractionation of the organic extracts

The organic extract was acetylated with a mixture of pyridine/acetic anhydride (1:1 v/v, 400 µl; 1 h, 60 °C). Following the addition of MeOH (1 mL), the solvents and the excess of reagent were removed under a flow of argon. The acetylated extract was treated with N,N-dimethylformamide dimethylacetal (150 µL) in toluene (1.5 ml) at 70 °C for 3 h in order to methylate the carboxylic acids. The formation of a dark precipitate was observed. The solvent-soluble part was recovered with a Pasteur pipette and the solvents were removed under a flow of argon, yielding the derivatized organic extract (16.5 mg). After treatment with activated copper to remove elemental sulfur, the derivatized extract was fractionated on a silica gel column eluting with 3 dead volumes of a mixture of DCM and ethylacetate (EtOAc) (8:2, v/v) to yield an apolar fraction (1.1 mg) analyzed using gas chromatography coupled to mass spectrometry (GC-MS).

3.2.2.3 GC-MS

GC-MS analyses were performed on a Thermo Scientific Trace Ultra gas chromatograph equipped with a programmed temperature vaporizing injector coupled to a Thermo Scientific TSQ Quantum mass spectrometer. The source was set at 220 °C and the mass spectrometer operated in the electron ionization mode at 70 eV and scanning *m/z* 50 to 700. Compound separation was performed on a HP5-MS column (30 m x 0.25 mm, 0.1 µm film thickness) using He as the carrier gas (constant flow, 1.1 mL/min). The oven temperature program was 70 °C (5 min),70 °C – 240 °C (4 °C/min), 240 °C – 300 °C (10 °C/min), and isothermal at 300 °C (20 min).

3.2.3 Preparation for radiocarbon dating of plant fibers

Fibers for dating were separated with tweezers from the sample collected within the concretion covering the anchor ring after extraction with organic solvents, (cf. 3.2.2.1). The fibers were then subjected to an acid-base-acid chemical cleaning in the Laboratoire de Mesure du Carbone 14. This treatment eliminates potential contaminations from carbonated and humic origin. After drying, 12.3 mg of clean sample were combusted at 835 °C for 5 h in the presence of 500 mg of CuO grains and an Ag wire. The pure CO_2 evolved from the combustion step was then reduced into graphitic carbon that was pressed to form a target for the ^{14}C measurements in the AMS facility (Dumoulin et al., 2017 and Moreau et al. 2013). The radiocarbon result was calibrated with the OxCal 4.4 software (Bronk Ramsey, 2009) using the IntCal20 calibration curve (Reimer et al., 2020). An amount of 0.66 mg of carbon could be extracted by combusting the sample, representing about 5% carbon content. Its relatively poor carbon content is related to the highly mineralized context characterized by concretion and metal.

4 Results

4.1 Analyses of the ring

4.1.1 Nature of the metal and manufacturing process

The metallographic study of the alloy matrix evidenced a homogeneous microstructure with very low carbon content (< 0.02 wt% C) on the whole surface of the cross-section (Figure 6). The composition of the slag inclusions obtained from the chemical analysis is shown in the supplemental material (Table S1). The multivariate treatment of the chemical data, which are the ratios of elements notified Xij in Figure 7, revealed two distinct chemical signatures indicative of the use of metal pieces from different smelting operations, and potentially from two different workshops, that were welded together. The distinction between signatures is more specifically linked to differences in ratios including CaO and K2O. The presence of two chemical signatures also supports the presence of a welding line that is hardly visible at the microscopic scale (Figure 7), and thus may reflect a particularly skilled smithing production.

The SI also contains significant phosphorus (P_2O_5 weighted average content of 1.6% and 1.2% for each iron piece), indicating the presence of this element in the metal that was not revealed by etching with the Oberhoffer's reagent (absence of "ghost structures"). This phosphorus content, even when low, could have had direct consequences for the behavior of the metal by making ferritic alloy less ductile (Stewart et al., 2000). It could also explain the low C content in the metal, as phosphorus hinders the incorporation of C into the iron (Buchwald, V. F., 2005). While the presence of phosphorus is usually not favorable for iron, it cannot be excluded that the use of this metal quality was suitable for manufacturing the

massive ring of the anchors, which needed to be sufficiently robust, as it was the principal component connecting the anchor to the ship.

The phosphorus content in the SI may also evidence the use of a rather phosphoric ore source for the smelting process. Phosphoric ore deposits are present in many active siderurgical places in the western Roman Empire (Pagès et al., 2022; Kaloyeros and Ehrenreich, 1990), and a future study on provenance where we would compare chemical signatures of traces elements would allow for the testing of various hypotheses regarding its origin.

4.1.2 Radiocarbon dating of the ring

The ferritic nature (< 0.02 wt % C) of the alloy does not usually allow a radiocarbon study of iron since no carburized zone was found. Nevertheless, the large size of the sample allowed us to take the required quantity (4–5 g for an alloy of 0.02 wt % C) in order to extract the expected minimal amount of carbon required. At this stage of investigation, it is not excluded either that recycled scrap iron (i.e., older iron) was used and welded with other pieces of metal to manufacture the object since at least two different metal pieces were detected in the sample. If it is not necessarily so, one ^{14}C sample was taken from within each metal piece (4 g each) to avoid mixing samples of possibly different dating. Quantities of carbon (0.3 mg and 0.1 mg respectively) were finally measured (Table 2). The very small mass of carbon led to a greater uncertainty for sample 62203. Overall, the two radiocarbon dates are fully coherent and can be dated to the 2nd century CE. This result also shows that the two metal pieces from different workshops are contemporary and that no recycling case can be detected from this investigation.

4.2 Analyses of the black layer and fibers

4.2.1 Fiber identification

Phytoliths (silica bodies produced by plants) were observed for most of the SEM pictures together with other anatomical features, such as epidermal cells with sinuous walls and simple pits (Figure 8a). These indicate that the remains came from a leaf or a stem of a monocotyledon plant (i.e., from a plant that does not produce wood). The long cells with sinuous walls are common to Gramineae, such as *Stipa* sp., Juncaceae and Cyperaceae (Gale and Cutler, 2000). The triangular shape of the remains seen in a transverse section is a diagnostic feature of Cyperaceae (Metcalfe, 1969). The stem and leaf epiderms of Cyperaceae such as *Cyperus* spp. or *Carex* spp. exhibit some short and long cells morphology closely related to the phytolith shape that could be seen preserved on the ring (Hameed et al., 2012). Other epidermal characters were observed, namely paracytic stomata (two guard cells), trichomes (hairs), and phytoliths of conical shape (Figure 8 b). Above all, the ridge-shaped phytoliths described by Metcalfe

(1971) were observed. Stevanato et al. (2019) more recently detected and described this phytolith shape on 11 genera of Cyperaceae under the naming cylindrical sulcate tracheids.

A phytolith reference collection, including Cyperaceae, was documented by Fernández Honaine et al. (2009). Many Cyperaceae phytoliths are consistent with the microbotanical remains that we observed on the ring. Their anatomical features are similar to those that appear in the University College of London's online reference collection (Phytolith taxa index), which include *Scirpus lacustris*. The fibers preserved on the ring most likely originate from a Cyperaceae stem or leaf. This family is well known for its fiber properties whose genera include *Carex* and *Cyperus*. Unfortunately, it is difficult to determine further the nature of these remains as most of the characters described above are shared at the family level.

4.2.2 Organic molecular investigation of the pitch and fibers

This molecular investigation aimed at determining whether the fabrics or ropes used for the puddening of the ring were impregnated with an organic substance, such as a resin or a pitch-based material, commonly in use ("tarring") in marine environments (e.g., Bailly, 2015). In addition, this examination provides further information concerning the botanical origin of the fabrics or rope used for the puddening of the ring. Thus, the lipids from the apolar part of the derivatized solvent extract of the sample were investigated using GC-MS.

The presence of diterpenoid biomarkers related to abietane (H1-5, A1, Figure 9) suggests that the organic substance corresponds to a resin or a pitch originating from conifers, specifically Pinaceae (e.g. Evershed et al., 1985; Colombini et al., 2003; Connan et Nissenbaum, 2003; Bailly, 2015, Bailly et al., 2016). These substances were commonly used to impregnate fabrics and ropes for the puddening of the anchor ring. The importance of mono- to triaromatic diterpenoid hydrocarbons, such as H1-4 relative to resin acids like A1 and the occurrence of methyl retene H5, suggests that this organic substance had undergone significant thermal stress. It can therefore be proposed that it corresponds to a conifer tar (i.e., pitch) and not to a resin (e.g., Evershed et al., 1985; Colombini et al., 2003; Connan et Nissenbaum, 2003; Bailly et al., 2016).

However, the sole presence of these aromatic compounds is generally not sufficient to demonstrate that the organic substance analyzed is a tar rather than a resin. Indeed, the majority of these compounds can also be formed by the diagenetic transformation of diterpenic acids (e.g., Simoneit et al., 1986; Reunanen et al., 1990; Martin et al., 1999). Nevertheless, a ratio of H1 relative to H2 of ca. 3/4 as observed in this case, corresponds to that generally found in pitch and not when H1 and H2 are formed by anaerobic diagenetic processes (large predominance of H2; Hynning et al., 1993; Tavendale et al., 1997; Martin et

al., 1999; Bailly, 2015; Bailly al., 2016). In addition, the methylated analogues of retene, such as H5, are frequently encountered in pitch and are not formed by early diagenetic transformation processes affecting resin acids (Bailly et al., 2016). The extremely low amounts of diterpenoids observed within the concretion that developed around the anchor ring could be explained by the destruction of most of the original organic material due to the unfavorable diagenetic conditions for preservation prevailing in the concretion.

The main compounds eluted at the end of the chromatogram can be divided into four main series comprising linear compounds (empty and filled triangles, Figure 9), steroids (S1, S2), triterpenes (T1-6), and phenolic derivatives (filled diamonds). These compounds are all typical biomarkers originating from land plants. *n*-Alkanes and *n*-alcohols are constituents of cuticular waxes widely distributed in the plant kingdom and are therefore not specific biomarkers. Nevertheless, their distribution can sometimes be interpreted in terms of botanical origin based on homologue predominance (e.g., Van Bergen et al., 1997; Trendel et al., 2010). Steroids are dominated by C_{29} sterols and stanols (S1, S2), which are typical plant biomarkers. The main triterpenes identified (T1-T6) are common and widely distributed in angiosperms and cannot be related to a more specific source. Finally, the phenolic compounds could not be unambiguously identified solely based on mass spectrometry and might be related to lignin derivatives.

All these compounds most likely originated from the fibers derived from the ropes used for the puddening of the ring and correspond to lipids from angiosperms. The distribution of these compounds is thus not incompatible with that expected for plants of the *Cyperaceae* family (see section 3.2.3). Yet they do not possess a specificity sufficient to relate them to a more precise botanical origin at the species or genus level. In addition, it is difficult to find in the literature comparative molecular distributions of organic extracts of sedges that might have been used in such a context. It appears that hemp can unambiguously be excluded as a possible vegetal source. Indeed, if the predominance of the C_{28} homologue among the *n*-alcohols is a typical feature of the organic extract of hemp ropes as is the presence of triterpenoids T1-T4 (Gutierrez et al., 2006; Bailly, 2015), the predominance of the C_{31} homologue among the *n*-alkanes from our sample is not compatible with this possibility since the C_{29} homologue predominates the *n*-alkane distribution from hemp extracts (Gutierrez et al., 2006; Bailly, 2015).

4.2.3 Radiocarbon dating of plant fibers

After calibration, a radiocarbon date of 1840 +/- 30 BP obtained from the sample gave two calendar intervals of 124–250 cal CE with 91.8% confidence and 295–310 cal CE with 3.6% confidence (Table 4). The range 124–250 cal CE is closer to the iron radiocarbon ages, which first confirms the chronological consistency of the set ring/puddening. Assuming a possible old-wood effect for the

radiocarbon dating of the iron, this range can be suggested for both the manufacture of the iron and the organics used for puddening, Concerning the anchor itself, the chronological data obtained for the ring and the puddening allows us for the determination of the date of its production before the 3rd century CE.

5 Discussion

The focus on the ring has brought forth significant material and evidence contributing to larger discussions about the technology of production of these large devices. The radiocarbon dating of both the carbon content of the wrought iron and the fibers (Figure 10) indicates that it was produced in the early imperial period. The proximity and similar morphology of the anchors invites us to consider that the dating of the ring was the same for both anchors. This dating fits well with their typology (Kapitän, 1984) and removes doubts regarding the ancient origin of these out-of-context finds. They were forged at a time when iron anchors progressively replaced wooden anchors with fixed lead stock (Gianfrotta, 1980; Sadania, 2017). Iron anchors with a removable stock probably saved space on ships, which was a clear advantage (Kapitän, 1984; Haldane, 1986a).

The two Roman iron anchors in La Grande Motte seem to be the largest to have ever been found. Out of the 354 iron anchors reported by Votruba (2014), only five of them measure over 300 cm. The most famous of this group was certainly the anchor found in Lake Nemi (35/47 CE). Covered by wooden sheathing, its shank is 361 cm long, and the object weighs 417 kg (Ucelli, 1950). A 350 cm-long iron anchor was also found on the starboard aft of the Sud-Lavezzi 2 shipwreck (Liou and Domergue, 1990). Its 220 cm-long iron stock still set into the shank indicates that the anchor was in use when the ship sank in the early 1st century CE. The ship carried on board another 240 cm-long iron anchor that was probably stored in the hold, as well as three additional wooden anchors found close to the bow, whose lead stocks range from 160.5 to 170 cm length and weigh between 200 and 250 kg (Liou and Domergue, 1990). Even though the excavation data regarding this shipwreck is insubstantial, the presence of a 350 cm-long iron anchor reveals that these large iron anchors were not specific to magnificent ships, such as the *Syracusia*, provided with eight iron anchors (Athenaeus, *Deipnosophistae* 5.208e) (Nowacki, 2002; Pomey and Tchernia, 2006; Castagnino Berlinghieri, 2010; Nantet, 2020b). Certainly, big anchors are expected to fit large merchantmen. Nonetheless, the Sud-Lavezzi 2 shipwreck reveals that even small ships could be fitted with such large anchors. As for the four iron anchors found in Marritza, the length of their shanks was respectively 270 cm, 290 cm, 310 cm, and 350 cm (Pallarés, 1986). The rope was still tied to their ring (Votruba, 2014), but the fact that they were not provided with a stock could indicate that they were stored onboard when the ship sank sometime between the end of the 1st and the middle of the 2nd century CE (Pallarés, 1986). The same reason would explain the absence of stock on the iron anchor found in Cabrera 4 shipwreck that is entirely preserved, which was loaded with lead ingots and

700 amphoras and dates to the early 1st century CE (Veny, 1979; Pons et al., 2001; Domergue et al., 2013). This anchor was 325 cm long with 180 cm arms-beam and was provided with a ring of 60 cm diameter. On the same shipwreck, the lower part of an iron shank (171 cm long) was also discovered. The absence of any hull does not allow us to draw conclusions on how sizable the ships outfitted with such large iron anchors would have been. The very low number of shipwrecks corresponding to large merchantmen that have been excavated makes it difficult to arrive at a definite answer, as no anchors have been found thus far from the few known examples, namely in La Madrague de Giens (75–60 BCE) (Tchernia et al., 1978; Pomey, 1982; Hesnard, 2012), Bou-Ferrer (1st cent. CE) (Juan Fuentes, 2018), and Caesarea (1st cent. CE) (Fitzgerald, 1994; Nantet, 2020a).

The technology required to manufacture these remarkable anchors in antiquity is particularly noteworthy. Speziale, who investigated the iron anchor found in Nemi, noticed that they would have necessitated advanced forging skills (Speziale, 1931; Votruba, 2014). The weld-bulge on the stem of a few anchors displays the precise location of the joint where the two parts meet, resulting from the crown-to-shank smithing process that consisted of working on the two separate pieces before the final assemblage (Votruba, 2014). The lower part of the shank found in Lake Nemi includes a similar bulge whose purpose would also have been to avoid the slippage of the shank inside the wooden sheathing (Sadania, 2017). The breaking points of both shanks discovered in Aigues-Mortes Bay are located slightly below their center, thus revealing a weak point due perhaps by the montage of the two iron portions, or a weld-bulge, that was not preserved.

The ring is a particular kind of element that is closely associated with the anchor. Subjected to all sorts of forces, it can be replaced (Sadania, 2017). Thus, this element can be of a much more recent date than the anchor to which it is attached. In any case, such heavy anchors as those found in La Grande-Motte probably would have required substantial cranes and devices for their lifting and handling. As the upper part of the hull is rarely preserved, the handling of such large specimens remains undocumented so far.

The two anchor finds may indicate that a ship sank at that location, although current investigations have not revealed any wreck. Following Kapitän's suggestion for the anchor found in Qawra Point (Maritime Museum, Vittoriosa, Malta), those from La Grande-Motte also may have served as stationary weights (Zammit, 1964; Kapitän, 1978; Frost 1982; Kapitän, 1984; Purpura, 2003; Azzopardi et al., 2012; Votruba, 2014; Sadania, 2017). But it seems unlikely to use iron anchors that were so complicated to manufacture and therefore not economical for a permanent anchorage site (Haldane, 1986a). It seems more likely that the anchors were lost. In any case, the presence of these two large anchors would indicate a mooring area established in relation to one of the numerous channels that led from the sea to the lagoons and marshes located along the coast that extends westward from the Rhône delta. The latter were too shallow to let in large merchantmen. In the imperial period, it was usual for big ships to anchor

445 at the entrance of channels, where their cargo would have been unloaded onto smaller vessels (Dionysius
446 3.44.3), like the *caudicariae* in Ostia (Boetto, 2008, 2016) or perhaps the example found in Mandirac
447 (Jézégou et al., 2015).
448
449 The most remarkable feature of the ring analysis is the pitch and fibers that remain under a concretion.
450 Pitch is obtained from trees of the Pinaceae family after heating, and molecular analysis rules out the
451 possibility of the use of bitumen. As for the plant fibers, they have been identified as Cyperaceae
452 (Cyperus canus) or sedge family, which are hydrophilic herbaceous reeds, known for their fibrous
453 properties, growing in wetlands in many parts of the world (clods, rivers and swamps, among other
454 environments). They possess high levels of salt tolerance and are therefore well suited to be used as
455 ropes on a ship. On the wreck of Ma'agan Mikhael (ca. 400 BCE), remnants of rope elements of the
456 Cyperaceae family (*Scirpus holoschoenus)* were found attached to the crown, the shank of the anchor,
457 and elsewhere on the ship (Charlton, 2003). These findings lead us to propose that what we found on La
458 Grande-Motte anchor constitutes a puddening. This practice of the wrapping of tarred fabrics bound
459 together with smaller ropes around the ring of an iron anchor was done in order to protect the cable from
460 chafing. It was still in use on modern sailing ships (Aubin, 1702; Martelli, 1838), which were provided
461 with hemp cables until the advent of chains in the early 19th century (Harland, 2013). So far, few anchors
462 have shown any signs of puddening, with two notable examples being the anchors of the *Mary Rose*
463 wrecked in 1545 (Votruba, 2014). Another particularly well-preserved example belonged to the HMS
464 *Dictator*, which had been commissioned in 1783 and broken up in 1817, evidences a ring overlaid with
465 a rope covered with canvas that had been pitched (Schwartz and Green, 1962). The anchor of the *Sydney*
466 *Cove* merchantman, lost in 1797, also showed a four-stranded laid rope, made of coir fiber or kayar,
467 which was built up from the short fibers of the outer husks of coconuts (Nash, 2002). Before our
468 discovery, this practice had not been evidenced yet for ancient anchors. An example of this is the study
469 of the rope that tied the Roman anchor of Maritza that did not detail whether it had been once connected
470 to the ring (Pallarés, 1986).
471
472 ## 6 Conclusion
473
474 The two largest finds evidence that imperial vessels moored in this bay. Our investigation has shown
475 that without obvious organic material, isolated iron anchors can be dated and are able to provide valuable
476 information about their manufacturing process. Radiocarbon analysis of the ring has provided a secure
477 range of dates that does not rely on a typology. A closer examination of the ring reveals the presence of
478 Cyperaceae plants that we have identified as the remains of small ropes that protected the cable from
479 chafing. The analyses we have carried out on the ring are even more significant and necessary as the
480 two iron anchors are the largest evidenced thus far for antiquity. For this reason, future investigation
481 should be extended to additional anchors of various dimensions, not only those found in shipwrecks but

also isolated finds. These would help to determine if several details underlined in the present study, namely the puddening, are specific and particular to these large devices or whether investigations of smaller examples could also reveal their presence. Our team's findings suggest that this method can complement chrono-typological and archaeo-metallurgical studies to date anchors out of archaeological context. There is great benefit to a close examination of the ring with combined techniques that offers promising perspectives for revealing anchors' manufacturing in antiquity that hitherto have not attracted sufficient attention.

Acknowledgements

Our thanks go to Max Guérout (GRAN/FED 4124) and Groupe de Recherche en Archéologie Navale, who conducted the operations. We are also grateful to Gregory Votruba for his precious advice. The probes were subsidized by Région Occitanie, Conseil Départemental de l'Hérault, DRASSM and CRESEM. The municipality of La Grande-Motte, the diving club La Palanquée, and the company Étrave Travaux, which extracted the anchor, provided superb logistical support for the underwater operations. Thanks are also due to Christophe Moulherat for taking SEM photos of the fibers and to Dana Katz for her editorial support in the preparation of the manuscript.

List of the figures

Figure 1: Location of the town of La Grande-Motte on the Aigues-Mortes Bay with the rivers and the principal ancient settlements located in the Roman province of Narbonensis (above) and the modern towns nearby (below). The green cross indicates the find site of the anchors (CAD: S. Berthaut-Clarac. Base map and data from OpenStreetMap and OpenStreetMap Foundation).

Figure 2: Plan of the excavation probes indicating the position of the anchors located at a 9 m depth and under 0.7 m of sediment (Drawing: M. Guérout, CAD: S. Berthaut-Clarac).

Figure 3: Reconstruction of anchors 1 and 2 (Drawing: A. Verra).

Figure 4: Picture of the sampled ring (Photo: Author).

Figure 5: Detection of small fibers located on the puddening of the ring (Photo: Author).

Figure 6 a): The collected anchor ring and visualization of the state of the metal corrosion at both cut ends. b): Cross-section of the sample and metallographic observation that highlight the ferritic nature of the ring.

Figure 7. Treatment of SI chemical data on the sample. a) Multivariate analysis of the compositional data–ratios of elements Xij- of the SI entrapped in the metal. Two chemical signatures (blue and violet) related to the smelting process are evidenced. b) The identified chemical signatures are reported in the

cross-section of the sample. The signatures are not mixed within the sample and each appears to be associated with a specific metal piece.

Figure 8: a) A fiber fragment observed by SEM: long cells of sinuous walls, simple pits are visible, b) the ridge-shaped (or cylindrical sulcate tracheids) phytoliths are visible all over the surface of the plant remains (SEM photo: Author, Quai Branly-Jacques Chirac Museum).

Figure 9: Gas chromatogram (GC-MS, EI, 70 eV) showing the distribution of lipid biomarkers from the organic extract of a sample collected within the concretion covering the anchor ring. Acids were analyzed as methyl esters and alcohols as acetates.

Figure 10: Graphical representation of the radiocarbon dating of iron and fibers

List of the tables

Table 1: Dimensions in cm of anchor 1 (C1/1, C1/2, C2) and anchor 2 (C3/1, C3/2), their preserved fragments, and reconstructed measurements, the latter of which are estimated due to the presence of concretions

Table 2: Radiocarbon dating results for the ring of anchor C3

Table 3: Anatomical characters observed with SEM

Table 4: Radiocarbon dating results for the fibers of anchor C3

Table S1 (supplementary material): Slag inclusion composition for detected compounds (weighted content). Contents normalized at 100%. S, Cl, Ti, V, Cr, Mn oxides were quantified but not presented in the table because their respective contents are always lower than 0.5%.

Classical Authors

Athenaeus, The Learned banqueters. 2, Books III.106e-V (edited and translated by S. Douglas Olson, 2006. Cambridge, Mass., Harvard University Press).

Dionysius of Halicarnassus, The Roman antiquities (trans. Earnest Cary and Edward Spelman, 1953. Cambridge, Mass., Harvard University Press).

Early modern printed sources

Aubin, N., 1702. Dictionnaire de marine contenant les termes de la navigation et de l'architecture navale avec les règles & proportions qui doivent y être observées. Amsterdam, Pierre Brunel.

Martelli, C., 1838. The Naval Officer's Guide for preparing ships for sea. London, Richard Bentley. 2nd edition.

555

556 **References**

557

558 Azzopardi, E., Gambin, T., Zerafa, R., 2012. Ancient anchors from Malta and Gozo. Malta
559 Archaeological Review 9, 22–31.
560
561 Bagan, G., Gailledrat, E., Jorda, C., 2010. Approche historique de la géographie des comptoirs
562 littoraux à l'Âge du Fer en Méditerranée occidentale à travers l'exemple du port de
563 Lattara (Lattes, Hérault). Quaternaire 21 (1), 85–100.
564 https://doi.org/10.4000/quaternaire.5470
565
566 Bailly, L., 2015. Caractérisation moléculaire et isotopique de goudrons et résines
567 archéologiques dérivés de conifères en contexte maritime. PhD Dissertation, University
568 of Strasbourg, France.
569
570 Bailly, L., Adam, P., Charrié, A., Connan, J., 2016. Identification of guaiacyl dehydroabietates
571 as novel markers of wood tar from Pinaceae in archaeological samples. Organic
572 Geochemistry 100, 80–88. https://doi.org/10.1016/j.orggeochem.2016.07.009
573
574 Bessac, J.C., 2002. Les carrières du Bois des Lens (Gard). Gallia 59, 29–51.
575 https://doi.org/10.3406/galia.2002.3095
576
577 Boetto, G., 2008. L'épave de l'Antiquité tardive Fiumicino 1: Analyse de la structure et étude
578 fonctionnelle. Archaeonautica 15, 29–62. https://doi.org/10.3406/nauti.2008.916
579
580 Boetto, G., 2016. Ancient Ports: The Geography of Connections, International Conference at
581 the Department of Archaeology and Ancient History, Uppsala University, 2010. Uppsala
582 University, 269–287.
583
584 Bronk Ramsey, C., 2009. Bayesian Analysis of Radiocarbon Dates. Radiocarbon 51, 337–360.
585 https://doi.org/10.1017/S0033822200033865
586
587 Buchwald, V. F., Wivel, H., 1998. Slag analysis as a method for the characterization and
588 provenancing of ancient iron objects. Materials Characterization 40 (2), 73-96.
589
590 Buchwald, V. F., 2005. Iron and steel in ancient times. The Royal Danish Academy of Sciences
591 and Letters, Copenhagen.
592
593 Castagnino Berlinghieri, E.F., 2010. Archimede alla corte di Hierone II: dall'idea al progetto
594 della della più grande nave del mondo antico, la Syrakosia. In: Braccesi, L., Raviolo, F.,
595 Sassatelli, G. (Eds.), Studi sulla grecità di Occidente, L'Erma di Bretschneider, Rome,
596 169–188 (Hesperia, 26).
597
598 Charlton, W.H. Jr, The rope and lashings. In: Linder, E., Kahanov, Y. (Eds), The Ma'agan
599 Mikhael ship. The recovery of a 2044-year-old merchantman, Israel Exploration Society,
600 Jerusalem, 134–139.
601

602 Ciarlo, N. C., Rosa, H. D., Elkin, D., Svoboda, H., Vázquez, C., Vainstub, D. et Perdiguero, L.
603 D., 2011. Examination of an 18th-century English anchor from Puerto Deseado (Santa
604 Cruz province, Argentina). Historical Metallurgy 45 (1), 17–25.
605
606 Colombini, M.P., Giachi. G., Modugno, F., Pallecchi, P., Ribechini, E., 2003. The
607 characterization of paints and waterproofing materials from the shipwrecks found at the
608 archaeological site of the Etruscan and Roman harbor of Pisa (Italy). Archaeometry 45,
609 659–674. https://doi.org/10.1046/j.1475-4754.2003.00135.x
610
611 Connan, J., Nissenbaum, A., 2003. Conifer tar on the keel and hull planking of the Ma'agan
612 Mikhael Ship (Israel, 5th century BC): identification and comparison with natural products
613 and artifacts employed in boat construction. Journal of Archaeological Science 30, 709–
614 719. https://doi.org/10.1016/S0305-4403(02)00243-1
615
616 Craddock, P., Wayman, M., Jull, A. J., 2002. The Radiocarbon Dating and Authentication of
617 Iron Artifacts. Radiocarbon 44, 717–732. https://doi.org/10.1017/S0033822200032173
618
619 Delqué-Količ, E., Leroy, S., Pagès, G., Leboyer, J., 2016. Iron Bar Trade between the
620 Mediterranean and Gaul in the Roman Period: ^{14}C Dating of Products from Shipwrecks
621 Discovered off the Coast of Saintes-Maries-de-la-Mer (Bouches-du-Rhône, France).
622 Radiocarbon 59 (2), 531–544. https://doi.org/10.1017/RDC.2016.109
623
624 Dillmann, P., L'Héritier, M., 2007. Slag inclusion analyses for studying ferrous alloys
625 employed in French medieval buildings: supply of materials and diffusion of smelting
626 processes. Journal of Archaeological Science 34, 1810–1823.
627 https://doi.org/10.1016/j.jas.2006.12.022
628
629 Disser, A., Dillmann, P., Bourgain, C., L'Héritier, M., Vega, E., Bauvais, S., Leroy, M., 2014.
630 Iron reinforcements in Beauvais and Metz Cathedrals: From bloomery or finery? The use
631 of logistic regression for differentiating smelting processes. Journal of Archaeological
632 Science 42, 315–333. https://doi.org/10.1016/j.jas.2013.10.034
633
634 Domergue, C., Quarati, P., Nesta, A., Piero Renato Trincherini, G.O., 2013. Les isotopes du
635 plomb et l'identification des lingots de plomb romains des mines de Sierra Morena.
636 Questions de méthode: l'exemple des lingots de l'épave Cabrera 4. Pallas 90, 243–256.
637 https://doi.org/10.4000/pallas.989
638
639 Dumoulin, J.-P., Comby-Zerbino, C., Delqué-Količ, E., Moreau, C., Caffy, S., Hain, S., Perron,
640 M., Thellier, B., Setti, V., Berthier, B., Beck, L., 2017. Status Report on Sample
641 Preparation Protocols Developed at the LMC14 Laboratory, Saclay, France: From
642 Sample Collection to ^{14}C AMS Measurement. Radiocarbon 59, 713–726.
643 https://doi.org/10.1017/RDC.2016.116
644
645 Eliyahu, M., Barkai, O., Goren, Y., Eliaz, N., Kahanov, Y. et Ashkenazi, D., 2011. The iron
646 anchors from the Tantura F shipwreck: typological and metallurgical analyses. *Journal*
647 *of Archaeological Science*, *38*(2), 233-245. https://doi.org/10.1016/j.jas.2010.08.023
648
649 Evershed, R.P., Jermna, K., Eglinton, G., 1985. Pine wood origin for pitch from the Mary Rose.
650 Nature 314, 528–530. https://doi.org/10.1038/314528a0

Fernández Honaine, M., Zucol, A, Osterrieth, M.L., 2009. Phytoliths of sedges from Pampean region, Argentina. Australian Journal of Botany 57 (6), 512–523. https://doi.org/10.1071/BT09041

Fitzgerald, M.A., 1994. The Ship. In: Oleson, J.P., Fitzgerald, M.A., Sherwood, A.N., Sidebotham, S., (Eds.). The Harbors of Caesarea Maritima; Results of the Caesarea Ancient Harbor Excavation Project 1980–85 II. Tempus Reparatum, Oxford, 163–223. (British Archaeological Reports, International Series 594).

Frost, H., 1970. Stone anchors as indications of early trade routes. In: M. Mollat (Ed.), Sociétés et compagnies de commerce en Orient et dans l'Océan Indien (Actes du huitième colloque international d'histoire maritime, Beyrouth, 5-10 Septembre 1966), SEVPEN, Paris, 55–61.

Frost, H., 1997. New thoughts on old anchors. In: Lazarov, M., Angelova, C. (Eds.), La Thrace et les sociétés maritimes anciennes. 18-24 september 1994 Sozopol, Thracia Pontica 6.1, 101–114.

Gale, R., Cutler, D.F., 2000. Plants in archaeology: identification manual of vegetative plant materials used in Europe and the Southern Mediterranean to c. 1500. Westbury Publications and Royal Botanic Gardens, Kew.

Gianfrotta, P.A., 1980. Ancore "romane". Nuovi materiali per lo studio dei traffici marittimi ("Roman" Anchors. New Materials for the Study of Maritime Traffic). Memoirs of the American Academy in Rome 36, 103–116. University of Michigan Press, Michigan. https://doi.org/10.2307/4238699

Gutiérrez, A., Rodígues, I.M., del Río, J.C., 2006. Chemical characterization of lignin and lipid fractions in industrial hemp bast fibers used for manufacturing high-quality paper pulps. Journal of Agricultural and Food Chemistry 54 (6), 2138–2144. https://doi.org/10.1021/jf052935a

Hameed, M., Nawaz, T., Ashraf, M., Tufail, A., Kanwal, H., Ahmad, M., Ahmad, I., 2012, Leaf anatomical adaptations of some halophytic and xerophytic sedges of the Punjab. Pakistan Journal of Botany 44 (1), 159–164.

Hadas, G., Liphschitz, N. and Bonani, G., 2005. Two Ancient Wooden Anchors from Ein Gedi, on the Dead Sea, Israel. International Journal of Nautical Archaeology 34 (2), 299–307. https://doi.org/10.1111/j.1095-9270.2005.00061.x

Haldane, D., 1986a, 12/10). Recent Discoveries about the Dating and Construction of Wooden Anchors. In: Les Thraces et les colonies grecques : VII - V s. av. n. è. Assotiation [i.e. Association] d'Etat 'Patrimoine Culturel et Historique, Sofia, 416–427, 555–557.

Haldane, D., 1986b. Wooden anchor arm construction. International Journal of Nautical Archaeology 15 (2), 163–166. https://doi.org/10.1111/j.1095-9270.1986.tb00567.x

Harland, J.H., 2013. The Transition from Hemp to Chain Cable: Innovations and Innovators, The Mariner's Mirror 99 (1), 72–85. https://doi.org/10.1080/00253359.2013.767000

Hesnard, A., 2012. L'épave la Madrague de Giens (Var) et la plaine de Fondi (Latium). Producteurs des vins, des amphores Dr. 1b et commerçants. Archaeonautica 17, 71–93.

Hüls, M., Grootes, P., Nadeau, M., 2011. Sampling Iron for Radiocarbon Dating: Influence of Modern Steel Tools on 14C Dating of Ancient Iron Artifacts. Radiocarbon 53 (1), 151–160. https://doi.org/10.1017/S0033822200034421

Hynning, P.A., Remberger, M., Neilson, A.H., Stanley, P., 1993. Identification and quantification of 18-nor- and 19- norditerpenes and their chlorinated analogues in samples of sediment and fish. Journal of Chromatography A 643, 439–452. https://doi.org/10.1016/0021-9673(93)80581-R

Jézégou, M.-P., Goodfellow, P.A., Letuppe, J., Sanchez, C., 2015. Underwater construction and maintenance: a wreck from Late Antiquity used to repair a breach in the bank of the Narbonne harbor channel Skyllis. Journal of Underwater Archaeology 15, 33–39.

Jézégou, M.-P., 2019. Forthcoming. Littoral d'Occitanie. Hérault. Au large de Mauguio. Trois sites de transport antique de matériaux de construction. Bilan scientifique du DRASSM 2019.

Jorda, C., Chabal, L., Blanchemanche, P., Fauduet, I., Odenhardt-Donvez, I., 2008. *Lattara* entre terres et eaux : paléogéographie et paléoboisements autour du port protohistorique. Gallia 65, 11–21.

Juan Fuentes, C., 2018. Una Interpretación Naútica a la Estiba del Cargamento en el Pecio Bou Ferrer. PHICARIA VI. Navegar el Mediterráneo. Mazarrón, Universidad Popular de Mazarrón. 131–145.

Kaloyeros, A.E., Ehrenreich, R.M., 1990. The Distribution of Phosphorus in Romano-British Ironwork. MRS Online Proceedings Library 185, 725–730. https://doi.org/10.1557/PROC-185-725

Kapitän, G., 1978. Exploration at Cape Graziano, Filicudi, Aeolian Islands, 1977. Results with annotations on the typology of ancient anchors. International Journal of Nautical Archaeology 7 (4), 269–277. https://doi.org/10.1111/j.1095-9270.1978.tb01077.x

Kapitän, G., 1984. Ancient anchors-technology and classification. International Journal of Nautical Archaeology 13, 33–44. https://doi.org/10.1111/j.1095-9270.1984.tb01175.x

Kapitän, G., 1994. Stone-shank anchors of the Arab-Indian trade period: Were they mooring anchors? The Bulletin of the Australian Institute for Maritime Archaeology 18 (2), 1–6.

Kuleff, I., Djingova, R., Alexandrova, A., Vakova, V., Amov, B., 1995. INAA, AAS, and lead isotope analysis of ancient lead anchors from the Black Sea. Journal of Radioanalytical and Nuclear Chemistry Articles 196 (1), 65–76. https://doi.org/10.1007/BF02036290

Leroy, S., Cohen, S. X., Verna, C., Gratuze, B., Téreygeol, F., Fluzin, P., Bertrand, L., Dillmann, P., 2012. The medieval iron market in Ariège (France). Multidisciplinary analytical approach and multivariate analyses. Journal of Archaeological Science 39 (4), 1080–1093. https://doi.org/10.1016/j.jas.2011.11.025

Leroy, S., Hendrickson, M., Delqué-Kolic, E., Vega, E., Dillmann, P., 2015a. First Direct Dating for the Construction and Modification of the Baphuon Temple Mountain in Angkor, Cambodia. PLoS ONE 10 (11): e0141052. https://doi.org/10.1371/journal.pone.0141052

Leroy, S., L'Héritier, M., Delqué-Kolic, E., Dumoulin, J-P., Moreau, C., Dillmann, P., 2015b. Consolidation or initial design? Radiocarbon dating of ancient iron alloys sheds light on the reinforcements of French Gothic Cathedrals. Journal of Archaeological Science 53, 190–201. https://doi.org/10.1016/j.jas.2014.10.016

Light, J. D., 1992. 16th century Basque ironworking: Anchors and nails. Materials Characterization 29 (2), 249–258. https://doi.org/10.1016/1044-5803(92)90119-3

Liou, B., Domergue, C., 1990. Le commerce de la Bétique au I^{er} siècle de notre ère. Archaeonautica 10, 11–123. https://doi.org/10.3406/nauti.1990.904

Martin, V.J., Yu, Z., Mohn, W.W., 1999. Recent advances in understanding resin acid biodegradation: microbial diversity and metabolism. Archives of Microbiology 172, 131–138. https://doi.org/10.1007/s002030050752

Metcalfe, C.R., 1969. Anatomy as an aid to classifying the Cyperaceae. American Journal of Botany 56 (7), 782–790. https://doi.org/10.1002/j.1537-2197.1969.tb09726.x

Metcalfe, C.R., 1971. Anatomy of the Monocotyledons: Vol. 5, Cyperaceae. Clarendon Press, Oxford.

Moll, F., 1927. The history of the anchor. The Mariner's Mirror 13 (4), 293–332. https://doi.org/10.1080/00253359.1927.10655436

Moreau, C., Caffy, I., Delqué-Količ, E., Dumoulin, J.-P., Hain, S., Quiles, A., Souprayen, C., Thellier, B., Vincent, J., 2013. Research and Development of the Artemis ^{14}C AMS Facility: Status Report. Radiocarbon 55, 331–337. https://doi.org/10.1017/S0033822200057441

Nantet, E., 2020a. Caesarea, Shipwreck. Preliminary Report, Hadashot Arkheologiyot. Excavations and Surveys in Israel 132.

Nantet, E., 2020b. The tonnage of the Syracusia: a metrological reconsideration. In Demesticha, S. and Blue, L. (Eds.), 'Under the Mediterranean' The Honor Frost Foundation Conference on Mediterranean Maritime Archaeology, 20th – 23rd October 2017 Short Report Series. https://doi.org/10.33583/utm2020.07

Nash, M., 2002. The Sydney Cove shipwreck project. International Journal of Nautical Archaeology 31 (1), 39–59.

Nowacki, H., 2002. Archimedes and ship stability. Max Planck Institute for the History of Science, Preprint 237.

Pagès, G., Dillmann, P., Vega, E., Berranger, M., Bauvais, S., Long, L., Fluzin, P. 2022 Vice-versa: The iron trade in the western Roman Empire between Gaul and the Mediterranean. PLoS ONE 17 (5): e0268209. https://doi.org/10.1371/journal.pone.0268209

Pallarés, F., 1986. Prime osservazioni sul relitto romano di Marritza. Bollettino d'arte. Archeologia subacquea 3, 75–80.

Pomey, P., 1982. Le navire romain de la Madrague de Giens. Comptes Rendus des Séances de l'Académie des Inscriptions et Belles-Lettres, 133–154.

Pomey, P., Tchernia, A., 2006. Les inventions entre l'anonymat et l'exploit: le pressoir à vis et la Syracusia. In: Lo Cascio, E. (Eds.), Innovazione Tecnica e Progresso Economico nel Mondo Romano. Atti degli Incontri Capresi di Storia dell'Economia Antica Capri 13-16 Aprile 2003, Edipuglia, Bari, 81–99.

Pons, V., Manuel, J., Frau, R., Magdalena, M., Rullan, M, R., 2001. Història i arqueologia de Cabrera. Palma de Mallorca, Ajuntament de Palma Ayuntamiento de Palma.

Purpura, G., 2003. Le Ancore. Archaeogate il portale Italiano di archeologia. Available at (accessed 27th February 2012).

Reimer, P.J., Austin, W.E.N., Bard, E., Bayliss, A., Blackwell, P.G., Ramsey, C.B., Butzin, M., Cheng, H., Edwards, R.L., Friedrich, M., Grootes, P.M., Guilderson, T.P., Hajdas, I., Heaton, T.J .,Hogg, A.G., Hughen, K.A., Kromer, B., Manning, S.W., Muscheler, R., Palmer, J.G., Pearson, C., Plicht, J. van der, Reimer, R.W., Richards, D.A., Scott, E.M., Southon, J.R., Turney, C.S.M., Wacker, L., Adolphi, F., Büntgen, U., Capano, M., Fahrni, S.M., Fogtmann-Schulz, A., Friedrich, R., Köhler, P., Kudsk, S., Miyake, F., Olsen, J., Reinig, F., Sakamoto, M., Sookdeo, A., Talamo, S., 2020. The IntCal20 Northern Hemisphere Radiocarbon Age Calibration Curve (0–55 cal kBP). Radiocarbon 62, 725–757. https://doi.org/10.1017/RDC.2020.41

Reunanen, M., Ekman, R., Heinonen, M., 1990. Long term alteration of pine tar in a marine environment. Holzforschung 44, 277–278. https://doi.org/10.1515/hfsg.1990.44.4.277

Sadania, M., 2017. Les ancres à jas de l'Antiquité au début du Moyen Âge sur le littoral français : première approche. In: Raux, S. (Ed.), Les modes de transport dans l'Antiquité et au Moyen Âge: mobiliers d'équipement et d'entretien des véhicules terrestres, fluviaux et maritimes, Editions Mergoil, Arles, 341–356.

Samuels, L. E. 1980. The metallography of a wrought iron anchor from the Bark Endeavor. Metallography 13 (4), 357–368. https://doi.org/10.1016/0026-0800(80)90032-4

Simoneit, B.R.T., Grimalt, J.O., Wang, T.G., Cox, R.E., Hatcher, P.G., Nissenbaum, A., 1986. Cyclic terpenoids of contemporary resinous plant detritus and of fossil woods, ambers and coals. Organic Geochemistry 10, 877–889. https://doi.org/10.1016/S0146-6380(86)80025-0

Schwartz, F. J. & Green, J., 1962. Found: One anchor from HMS Dictator. Maryland Historical Magazine, 57 (4), 367–370.

Speziale, G.C., 1931. The roman anchors found at Nemi. The Mariner's Mirror 17, 309–320. https://doi.org/10.1080/00253359.1931.10655619

Steiner, B.L., Alonso, N., Grillas, P., Jorda, C., Piquès, G., Tiller, M., Rovira, N., 2020. Languedoc lagoon environments and man: Building a modern analogue botanical macroremain database for understanding the role of water and edaphology in sedimentation dynamics of archaeobotanical remains at the Roman port of Lattara (Lattes, France). PLOS ONE 15(6): e0234853. https://doi.org/10.1371/journal.pone.0234853

Stevanato, M., Rasbold, G. G., Parolin, M., Luz, L. D., Lo, E., Weber, P., ... & Caxambu, M. G. 2019. New characteristics of the papillae phytolith morphotype recovered from eleven genera of cyperaceae. Flora 253, 49–55.

Stewart, J.W., Charles, J.A., Wallach, E.R., 2000. Iron–phosphorus–carbon system: Part 1 – Mechanical properties of low carbon iron–phosphorus alloys. Materials Science and Technology 16 (3), 275–282. https://doi.org/10.1179/026708300101507839

Tavendale, M.H., McFarlane, P.N., Mackie, K.L., Wilkins, A.L., Langdon, A.G., 1997. The fate of resin acids – 2. The fate of resin acids and resin acid derived neutral compounds in anaerobic sediments. Chemosphere 35 (10), 2153–2166. https://doi.org/10.1016/S0045-6535(97)00294-4

Tchernia A., Pomey, P., Hesnard, A., 1978 L'épave romaine de la Madrague de Giens, Var : campagnes 1972–1975: fouilles. Institut d`archéologie méditerranéenne. Aix-en-Provence, Bouches-du-Rhône.

Trendel, J.M., Schaeffer, P., Adam, P., Ertlen, D., Schwartz, D., 2010. Molecular characterisation of soil surface horizons with different vegetation in the Vosges Massif (France). Organic Geochemistry 41 (9), 1036-1039. https://doi.org/10.1016/j.orggeochem.2010.04.014

Ucelli, G., 1950. Le navi di Nemi. La Libreria dello Stato, Rome.

Van Bergen, P.F., Bull, I.D., Poulton, P.R., Evershed, R.P., 1997. Organic geochemical studies of soils from Rothamsted classical experiments – I. Total lipid extracts, solvent insoluble residues and humic acids from Broadbalk Wilderness. Organic Geochemistry 26, 117-135. https://doi.org/10.1016/S0146-6380(96)00134-9

Van der Merwe N. J., Stuiver M., 1968. Dating iron by the carbon-14 method. Current Anthropology 9 (1), 48–53.

Veny, C., 1979, Nuevos materiales de Moro Boti. Trabajos de Prehistoria 36, 465–488.

Votruba, G.F., 2014. Iron Anchors and Mooring in the Ancient Mediterranean (until ca. 1500 CE) (PhD thesis). The University of Oxford, Oxford.

Votruba, G.F., 2019. Building upon Honor Frost's Anchor-Stone Foundations. In: Blue, L. (Ed.), In the Footsteps of Honor Frost. The life and legacy of a pioneer in maritime archaeology. Sidestone Press, Leiden, 213-244.

Zammit, C.G., 1964. Underwater Archaeology. Report of the Working of the Museum Department for the Year 1963 (Malta).

1. Website references, accessed February 2022

Poaceae *Phragmites australis*. University College of London phytolith database. http://www.homepages.ucl.ac.uk/~tcrndfu/phytoliths/Phragmites%20australis/target2.html (Accessed August 2021)

Stipa capillata. University College of London phytolith database. http://www.homepages.ucl.ac.uk/~tcrndfu/phytoliths/Stipa%20Capilata/target3.html (Accessed August 2021)

Cyperaceae *Cyperus rotundus*. University College of London phytolith database. http://www.homepages.ucl.ac.uk/~tcrndfu/phytoliths/Cyperus%20rotundus/target3.html (Accessed August 2021)

Scirpus lacustris a. University College of London phytolith database. http://www.homepages.ucl.ac.uk/~tcrndfu/phytoliths/Scirpus%20lacustris%20infl/target3.html (Accessed August 2021)

Scirpus lacustris b. University College of London phytolith database. http://www.homepages.ucl.ac.uk/~tcrndfu/phytoliths/Scirpus%20lacustris%20infl/target17.html (Accessed August 2021)

Cyperus L. Plants of the World Online, Royal Botanic Garden Kew. http://powo.science.kew.org/taxon/urn:lsid:ipni.org:names:330001-2

Table 1: Dimensions in cm of anchor 1 (C1/1, C1/2, C2) and anchor 2 (C3/1, C3/2), their preserved fragments, and reconstructed measurements, the latter of which are estimated due to the presence of concretions

Dimensions (in cm)	**Anchor 1**			**Anchor 2**		
	C1/1 + C1/2 Preserved	C2 Preserved	**Overall C1+C2 Reconstructed**	C3/1 Preserved	C3/2 Preserved	**Overall C3 Reconstructed**
Length of shank	258	117	**375**	254	116	**370**
Length of stock	293	-	**293**	228	-	**228**
Length of arms	-	112 (right arm) 116 (left arm)	**112 (right arm)** **116 (left arm)**	-	108 (left arm)	**108 (left arm)**
Arm-beams		185	**185**	-	180	**180**
Diameter of cable-ring (outer/inner)	32/24	-	**32/24**	35/23	-	**35/23**

Table 2: Radiocarbon dating results for the ring of anchor C3

Sample name	Lab.ID	Extracted carbon content (mg)	$\delta^{13}C$ (‰)	Radiocarbon age (BP, 1 σ)	Calibrated age (2σ, 95.4%)
GDM20-org-1a	SacA 62202	0.28	-31.2	1940 ± 30	10 CE–204 CE
GDM20-org-1b	SacA 62203	0.11	-31.4	1960 ± 50	46 BCE–206 CE

Table 3: Anatomical characters observed with SEM

SEM Picture	Long cells	Short cells	Cell walls	Pits	Stomata	Phytoliths
MEB-02	Rectangular	Round	Sinuous	Round	Paracytic	Saddle
MEB-03	Rectangular	-	Sinuous	Simple 5 µm	-	Bride-shaped
MEB-04	-	-	Sinuous	-	-	Saddle and bridge-shaped
MEB-05	-	-	-	-	-	Bride-shaped

Table 4: Radiocarbon dating results for the fibers of anchor C3

Sample name	Lab. ID	$\delta^{13}C$ (‰)	Radiocarbon age (BP, 1σ)	Calibrated age (2σ, 95.4%)
GDM20-org-fibers	SacA 64799	−22.5	1840 ± 30	124 CE (91.8%) 250 CE 295 CE (3.6%) 310 CE

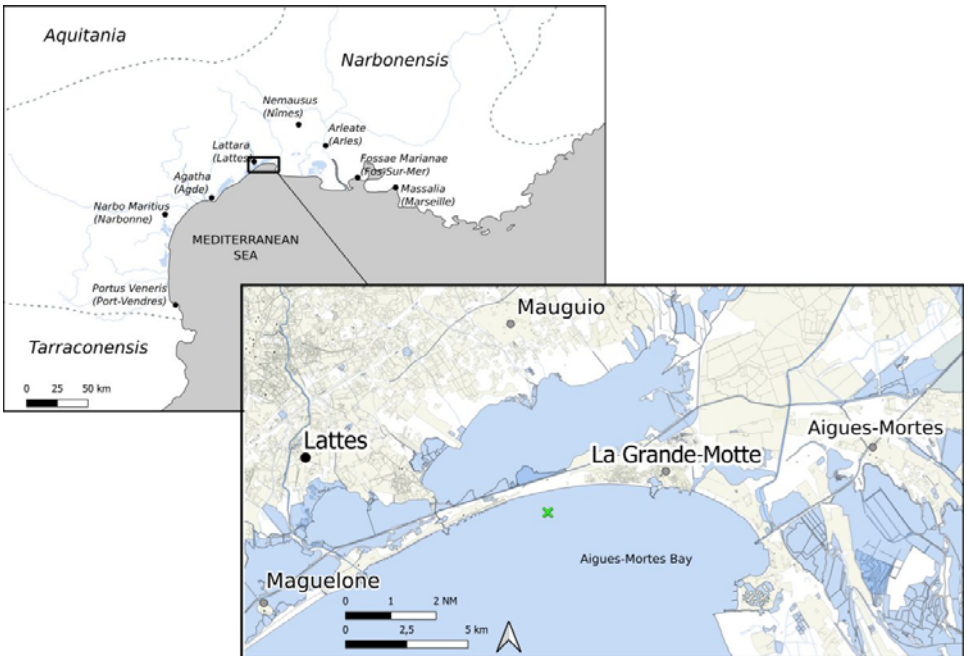

Figure 1: Location of the town of La Grande-Motte on the Aigues-Mortes Bay with the rivers and the principal ancient settlements located in the Roman province of Narbonensis (above) and the modern towns nearby (below). The green cross indicates the find site of the anchors (CAD: S. Berthaut-Clarac. Base map and data from OpenStreetMap and OpenStreetMap Foundation).

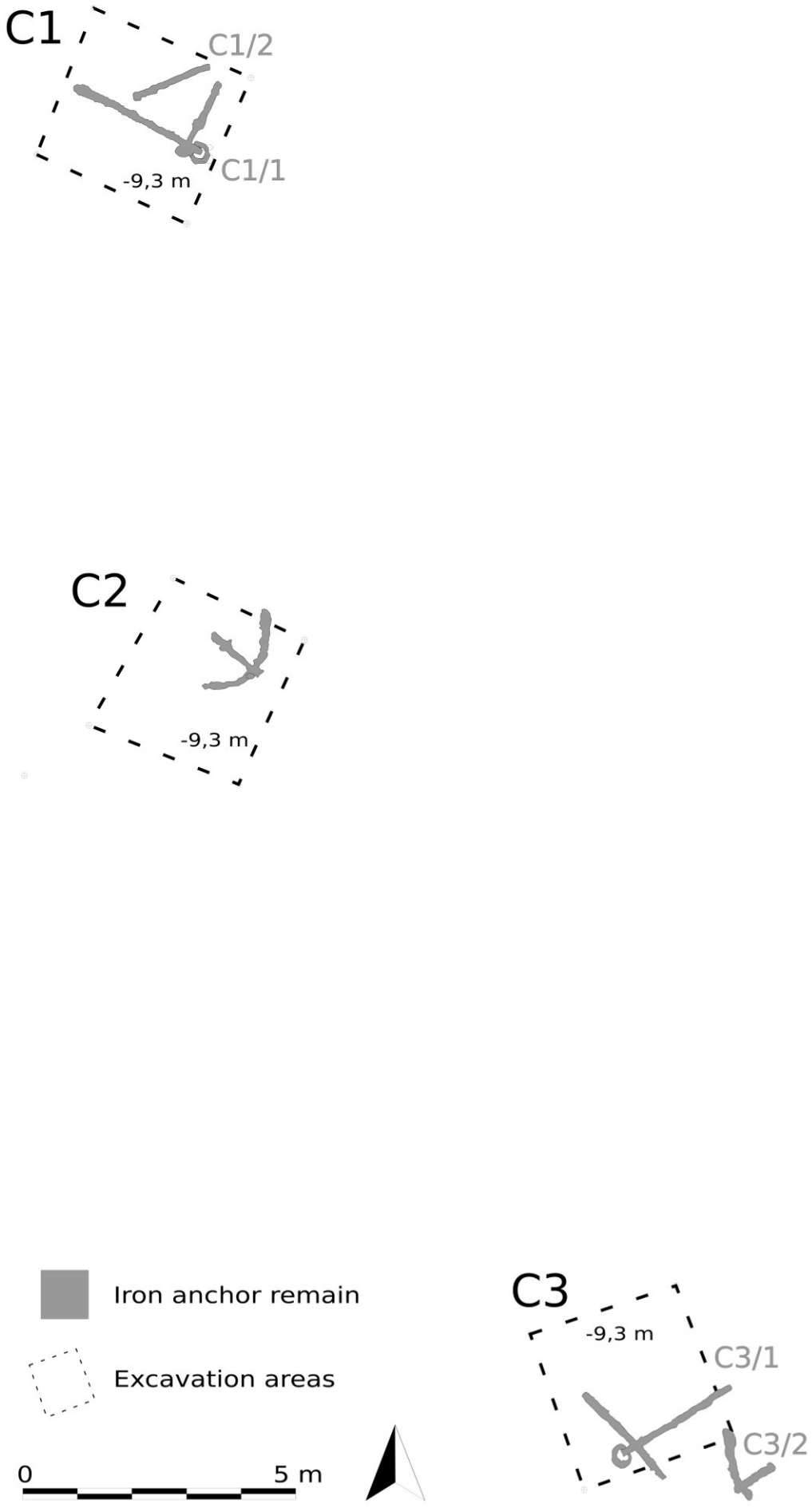

Figure 2: Plan of the excavation probes indicating the position of the anchors located at a 9 m depth and under 0.7 m of sediment (Drawing: M. Guérout, CAD: S. Berthaut-Clarac).

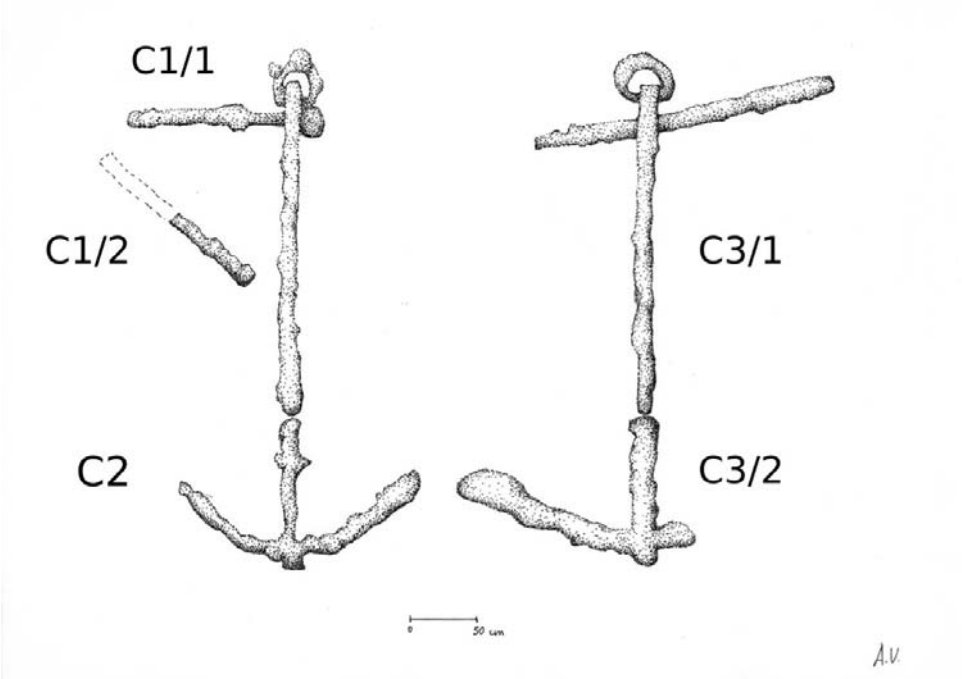

Figure 3: Reconstruction of anchors 1 and 2 (Drawing: A. Verra).

Figure 4: Picture of the sampled ring (Photo: Author).

Figure 5: Detection of small fibers located on the puddening of the ring (Photo: Author).

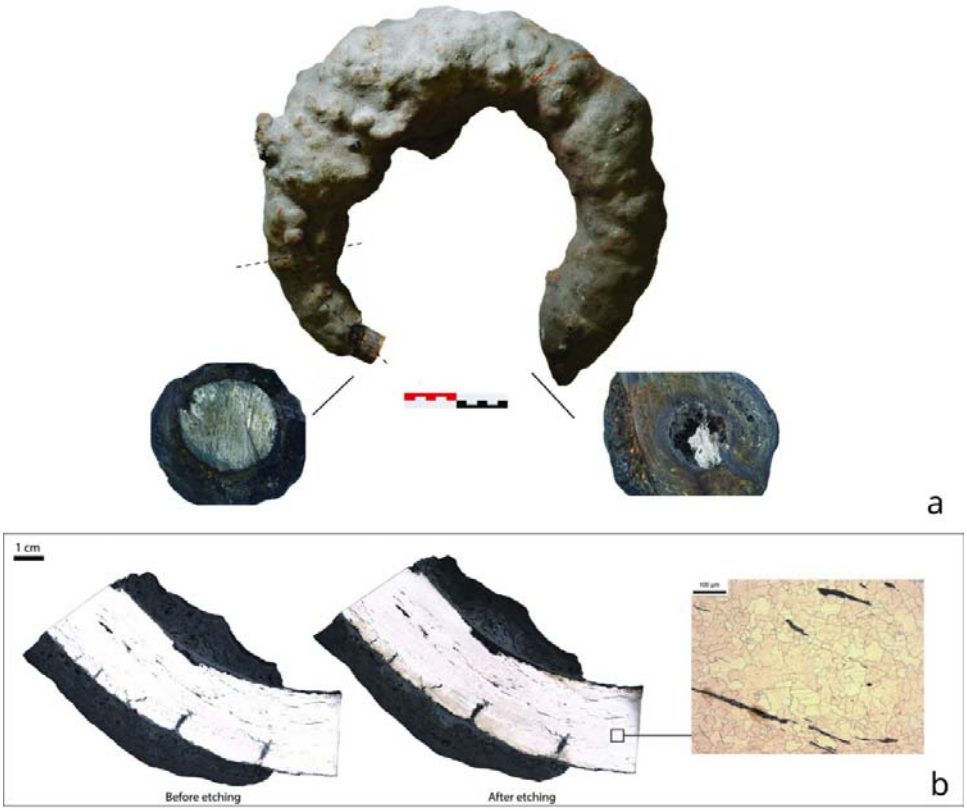

Figure 6 a): The collected anchor ring and visualization of the state of the metal corrosion at both cut ends. **b)**: Cross-section of the sample and metallographic observation that highlight the ferritic nature of the ring.

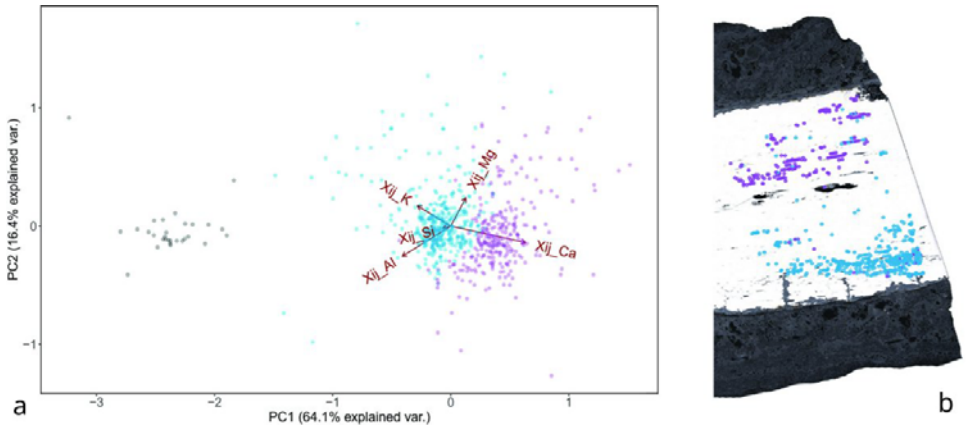

Figure 7: Treatment of SI chemical data on the sample. a) Multivariate analysis of the compositional data–ratios of elements Xij- of the SI entrapped in the metal. Two chemical signatures (blue and violet) related to the smelting process are evidenced. b) The identified chemical signatures are reported in the cross-section of the sample. The signatures are not mixed within the sample and each appears to be associated with a specific metal piece**.**

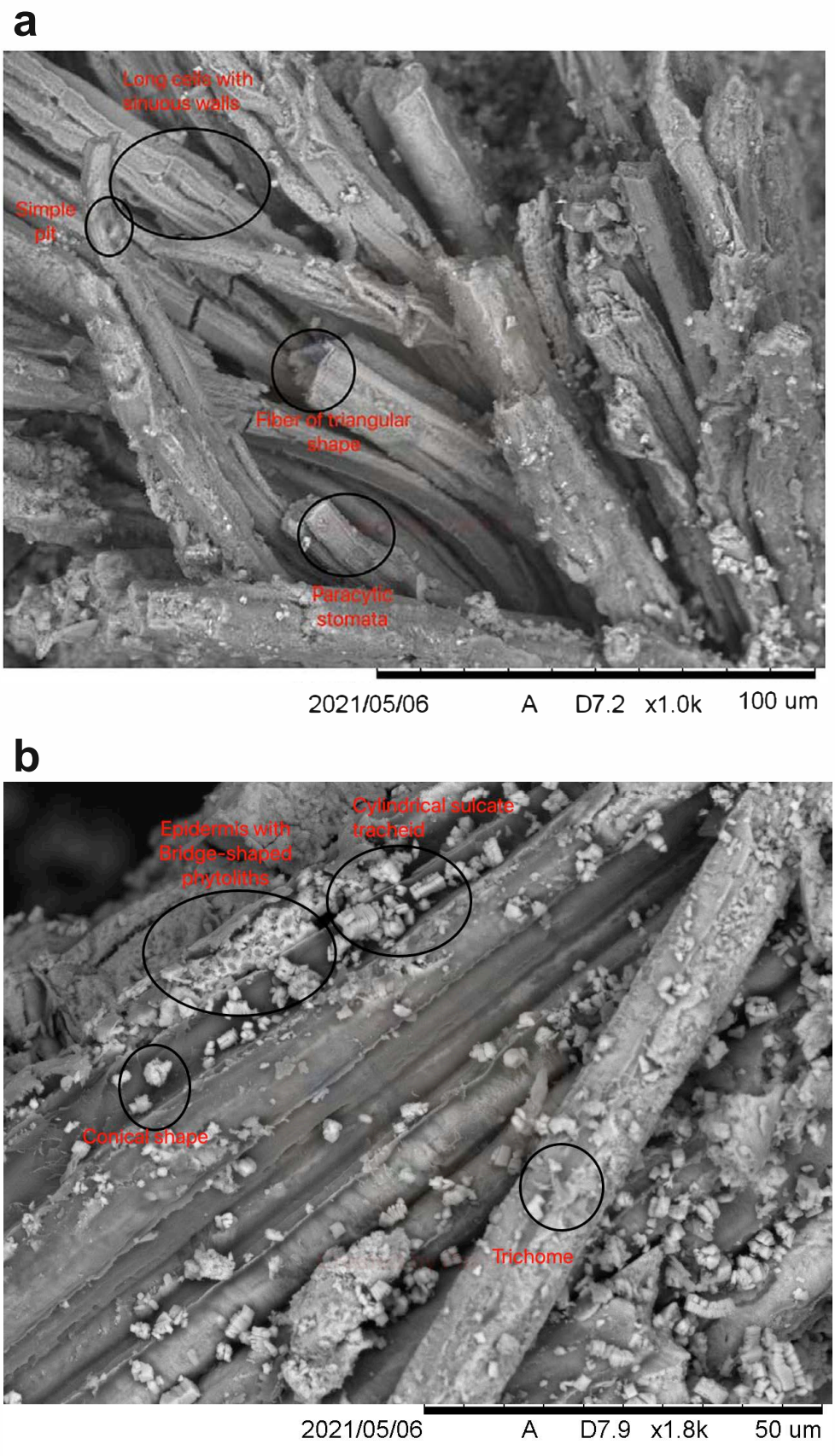

Figure 8: **a)** A fiber fragment observed by SEM: long cells of sinuous walls, simple pits are visible, **b)** the ridge-shaped (or cylindrical sulcate tracheids) phytoliths are visible all over the surface of the plant remains (SEM photo: Author, Quai Branly-Jacques Chirac Museum).

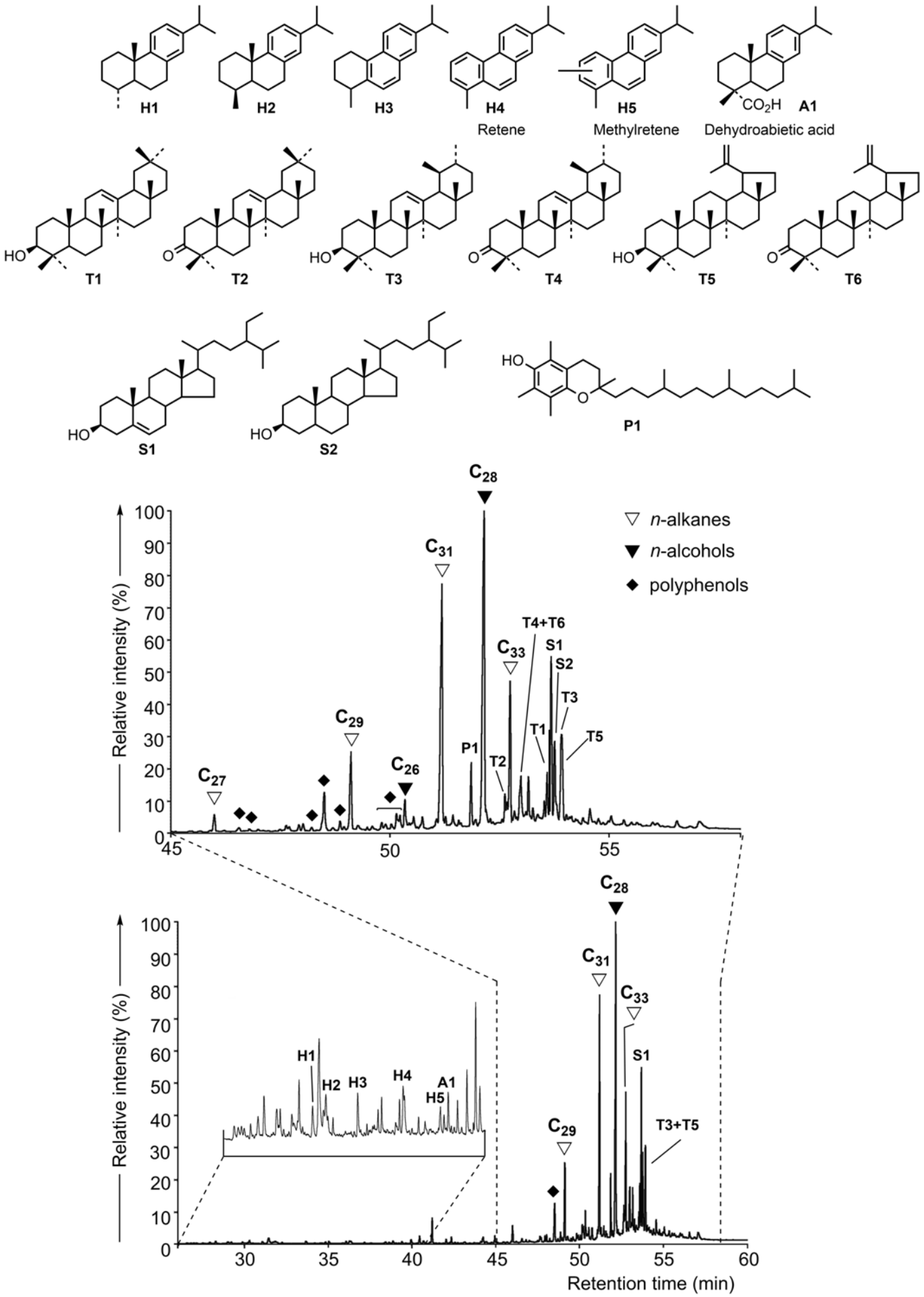

Figure 9: Gas chromatogram (GC-MS, EI, 70 eV) showing the distribution of lipid biomarkers from the organic extract of a sample collected within the concretion covering the anchor ring. Acids were analyzed as methyl esters and alcohols as acetates.

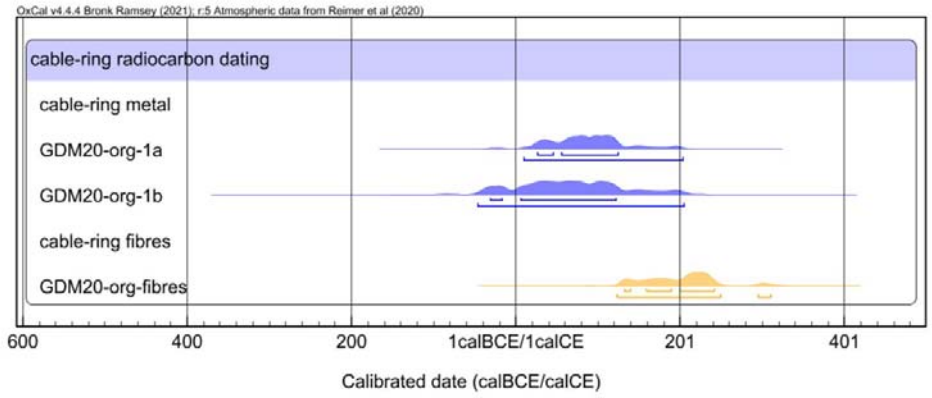

Figure 10: Graphical representation of the radiocarbon dating of iron and fibers